Published in final edited form as:
Cell Metab. 2012 May 2; 15(5): 739–751. doi:10.1016/j.cmet.2012.03.002.

Calcium signaling through CaMKII regulates hepatic glucose production in fasting and obesity

Lale Ozcan[1], **Catherine C.L. Wong**[2], **Gang Li**[1], **Tao Xu**[2], **Utpal Pajvani**[1], **Sung Kyu Robin Park**[2], **Anetta Wronska**[3], **Bi-Xing Chen**[3], **Andrew R. Marks**[1,3], **Akiyoshi Fukamizu**[4], **Johannes Backs**[5], **Harold A. Singer**[6], **John R. Yates III**[2], **Domenico Accili**[1], and **Ira Tabas**[1,3,7,*]

[1]Department of Medicine, Columbia University, New York, NY 10032, USA

[2]Department of Chemical Physiology, Scripps Research Institute, La Jolla, CA 92037, USA

[3]Department of Physiology & Cellular Biophysics and The Clyde and Helen Wu Center for Molecular Cardiology, Columbia University, New York, NY 10032, USA

[4]Life Science Center, Tsukuba Advanced Research Alliance, University of Tsukuba, Tsukuba, Japan

[5]Department of Internal Medicine III, University of Heidelberg, Heidelberg, Germany

[6]Center for Cardiovascular Sciences, Albany Medical College, Albany, NY 12208 USA

[7]Department of Pathology & Cell Biology, Columbia University, New York, NY 10032, USA

SUMMARY

Hepatic glucose production (HGP) is crucial for glucose homeostasis, but the underlying mechanisms have not been fully elucidated. Here we show that a calcium-sensing enzyme, CaMKII, is activated in a calcium- and IP3R-dependent manner by cAMP and glucagon in primary HCs and by glucagon and fasting *in vivo*. Genetic deficiency or inhibition of CaMKII blocks nuclear translocation of FoxO1 by affecting its phosphorylation, impairs fasting- and glucagon/cAMP-induced glycogenolysis and gluconeogenesis, and lowers blood glucose levels, while constitutively active CaMKII has the opposite effects. Importantly, the suppressive effect of CaMKII deficiency on glucose metabolism is abrogated by transduction with constitutively nuclear FoxO1, indicating that the effect of CaMKII deficiency requires nuclear exclusion of FoxO1. This same pathway is also involved in excessive HGP in the setting of obesity. These results reveal a calcium-mediated signaling pathway involved in FoxO1 nuclear localization and hepatic glucose homeostasis.

*Correspondence: iat1@columbia.edu.

SUPPLEMENTAL INFORMATION

Supplemental Information includes 5 supplemental figures distributed among 7 pages and Supplemental Experiment Procedures, and the website at http://fields.scripps.edu/published/foxo1_Tabas_2012/) includes raw mass spectrometry data and parameter files; Tables S1 and S2 showing phospho-peptide coverage of FoxO1 isolated from WT and *Camk2g*$^{-/-}$ HCs; and annotated tandem mass spectra for WT peptides 7, 10, and 11 (3 figures in supple_S1.pptx).

INTRODUCTION

Liver is the main organ responsible for maintaining euglycemia under conditions of nutrient deprivation. During the early stages of fasting, liver uses glycogen stores to mobilize glucose (Radziuk and Pye, 2001). As fasting progresses, de novo synthesis of glucose from non-carbohydrate precursors, gluconeogenesis, becomes the main contributor to hepatic glucose production (HGP) (Lin and Accili, 2011). These changes occur rapidly in response to direct hormonal signaling. In addition, both insulin and glucagon affect transcription of glucose-6-phosphatase (*G6pc*), which is involved in both gluconeogenesis and glycogenolysis, and phosphoenolpyruvate carboxykinase (*Pck1*), which also regulates HGP (Pilkis and Granner, 1992; Burgess et al., 2007). During fasting, changes in the subcellular localization of "glucogenic" transcription factors, such as FoxO (1, 3, and 4) and Crct2, activate expression of these genes (Lin and Accili, 2011). In addition, different co-activators, such as peroxisome proliferator-activated receptor-γ oactivator-1α (PGC-1α) and CBP, are thought to interact with components of the cAMP response, including CREB, hepatic nuclear factor 4α (HNF4α), Sirt1, and Clock genes, leading to an increase in transcription of gluconeogenic genes (Hall et al., 1995; Matsumoto et al., 2007; Puigserver et al., 2003; Rhee et al., 2003). In addition to its role in stimulating HGP during fasting, excessive glucagon signaling is thought to play an important role in hyperglycemia in type 2 diabetes (Sorensen et al., 2006; Unger and Cherrington, 2012; Saltiel, 2001).

The intracellular signal transduction pathways through which glucagon stimulates the nuclear translocation of HGP transcription factors in general, and FoxO1 in particular, to stimulate HGP is not well understood. In this context, we became interested in previous reports that linked intracellular calcium (Ca^{2+}_i) to the regulation of gluconeogenesis (Friedmann and Rasmussen, 1970; Kraus-Friedmann and Feng, 1996; Marques-da-Silva et al., 1997). For example, glucagon and cAMP can increase Ca^{2+}_i, and Ca^{2+}_i chelation has been shown to reduce glucagon induced HGP gene expression and glucose production (Bygrave and Benedetti, 1993; Staddon and Hansford, 1989; Mine et al., 1993). Based on these previous studies, which did not offer a molecular mechanism linking Ca^{2+}_i to hepatic glucose metabolism, we conceived a hypothesis implicating a role for the Ca^{2+}_i -sensing enzyme CaMKII.

Calcium calmodulin-dependent kinase II (CaMKII) is a serine–threonine kinase that is an important mediator of Ca^{2+}_i signaling in cells (Couchonnal and Anderson, 2008; Singer, 2011). There are four CaMKII isoforms—α, β, γ and δ—each encoded by a separate gene. The α and β isoforms are mostly neuronal, while CaMKIIγ and δ are expressed in a wide variety of tissues. After binding calcium/calmodulin complex, autophosphorylation on Thr287 results in calcium/calmodulin independent activity (Couchonnal and Anderson, 2008; Singer, 2011). Most studies on CaMKII have been carried out in neurons and cardiomyocytes, and there is only a limited understanding of CaMKII in other tissues, with none to date related to glucose metabolism. In the present study, we show that CaMKII activity is increased by cAMP and glucagon and also in response to fasting *in vivo*. We further demonstrate that CaMKII plays an essential role in the regulation of glycogenolysis and gluconeogenesis. In particular, we provide evidence that CaMKII has a profound effect on FoxO1 nuclear localization in a manner that regulates the expression of two key enzymes, *G6pc* and *Pck1*, *in vitro* and *in vivo*. Finally, we present evidence suggesting that this same pathway is involved in excessive HGP in the setting of obesity.

RESULTS

Glucagon and fasting activate hepatic CaMKII in a IP3R- and Ca^{2+}_i-dependent manner

Glucagon has been shown to increase intracellular calcium (Ca^{2+}_i) in hepatocytes (HCs) (Staddon and Hansford, 1989), which we recently verified (Y. Wang, G. Li, J. Goode, J. C. Paz, R. Screaton, W. H. Fischer, I. Tabas, and M. Montminy, manuscript submitted for publication). To determine whether glucagon activates the Ca^{2+}_i-sensing enzyme, CaMKII, we treated primary murine HCs with glucagon for various periods of time and then assayed CaMKII enzymatic activity and CaMKII phosphorylation at Thr287, which is a measure of its activation state (Couchonnal and Anderson, 2008; Singer, 2011). The results of both assays show that CaMKII activity increases as a function of time of glucagon treatment (Figure 1A–B). We used the cytosolic calcium chelator,1,2-bis[2-aminophenoxy]ethane-N,N,N',N'-tetraacetic acid tetrakis [acetoxymethyl ester] (BAPTA-AM), to determine the role of Ca^{2+}_i on CaMKII activation and found that BAPTA-AM markedly decreased glucagon-induced CaMKII phosphorylation (Figure 1C).

Inositol 1,4,5-trisphosphate receptor (IP_3R) channels, located in the endoplasmic reticulum (ER), release Ca^{2+} in response to IP_3 binding and play a major role in intracellular Ca^{2+}_i homeostasis. Additional studies have revealed that glucagon-induced PKA phosphorylates and increases IP3R activity, leading to an increase in Ca^{2+}_i (Y. Wang, G. Li, J. Goode, J. C. Paz, R. Screaton, W. H. Fischer, I. Tabas, and M. Montminy, manuscript submitted for publication). Glucagon has also been shown to induce phospholipase C-mediated IP3 release (Hansen et al., 1998). To investigate the contribution of IP3Rs in glucagon-induced CaMKII activation, we used the IP3R inhibitor xestospongin C and, as a complementary approach, adeno-Cre-treated HCs from *Ip3r1*$^{fl/fl}$ mice. Both xestospongin C treatment and Cre-mediated deletion of IP3R1 led to a significant decrease in glucagon-induced CaMKII phosphorylation, demonstrating the critical role of IP3Rs in this process (Figure 1D).

Glucagon receptor signaling, including that involved in the increase in Ca^{2+}_i (Staddon and Hansford, 1989), is mediated by activation of adenylate cyclase to produce cAMP, followed by activation of protein kinase A (PKA), a key enzyme involved in HGP. In this context, we found that treatment of HCs with 8-bromo-cAMP mimicked the effect of glucagon and led to a marked increase in phospho-CaMKII (Figure 1E). Moreover, when HCs were treated with the PKA inhibitor H89 prior to the addition of glucagon, glucagon-mediated increase in phospho-CaMKII was markedly inhibited (Figure 1F). These data support the existence of a pathway in which glucagon-cAMP-PKA signaling promotes phosphorylation/activation of CaMKII through its effects on IP3R-mediated intracellular Ca^{2+} release.

To examine whether CaMKII is regulated by glucagon *in vivo*, we challenged mice with a bolus of intraperitoneal (i.p.) glucagon. Consistent with the effects observed in cultured HCs, hepatic CaMKII phosphorylation was induced by glucagon treatment (Figure 1G). We found that a glucagon dose as low as 1 μg kg^{-1} was capable of phosphorylating CaMKII in the liver (Figure S1A). To gain *in vivo* evidence that IP3Rs are important in the regulation of glucagon-mediated CaMKII phosphorylation, we treated mice with i.p. xestospongin C for 4 days. The mice were then challenged with glucagon, and liver extracts were assayed for p-CaMKII. As shown in Figure 1H, xestospongin C treatment markedly reduced glucagon-induced CaMKII phosphorylation. Next, we compared hepatic CaMKII phosphorylation during the transition from a fed to fasting state, which is known to elevate plasma glucagon (Lin and Accili, 2011) (Figure S1B). The data show that hepatic CaMKII phosphorylation was significantly increased upon fasting, whereas the total amount of CaMKII appeared to be unaffected by nutrient status (Figure 1I). Moreover, upon re-feeding, the level of p-CaMKII in liver diminished (Figure 1J). As with glucagon treatment, fasting-induced phosphorylation of CaMKII was suppressed by xestospongin C treatment of

the mice (Figure S1C). These data show that activity of hepatic CaMKII is regulated by nutrient status in a manner that is consistent with a potential role in fasting-induced HGP.

CaMKII promotes glucose production in primary HCs

CaMKIIγ is the major CaMKII isoform in HCs, and the other isoforms are not induced in HCs lacking the γ isoform (Figure 2A). In view of the regulation of hepatic CaMKII activity by glucagon and fasting *in vivo*, we assayed glucose production in HCs from WT and *Camk2g*$^{-/-}$ mice. We examined the cells under basal conditions and after stimulation with forskolin, a glucagon mimetic and a potent adenylate cyclase activator (Harano et al., 1985). The data show that both basal and forskolin-induced glucose production was suppressed in CaMKIIγ-deficient HCs (Figure 2B). We next examined glucose production in WT HCs transduced with adenoviruses expressing constitutively active CaMKII (adeno-CA-CaMKII), "kinase-dead" dominant-negative CaMKII (adeno-KD-CaMKII) (Pfleiderer et al., 2004), or LacZ control. CA-CaMKII possesses an amino acid substitution, T287D, which mimics autophosphorylation at T287 and results in autonomous activity in the absence of bound calcium/calmodulin, while KD-CaMKII has a disabling mutation in the kinase domain (Pfleiderer et al., 2004). We observed an increase in both basal and forskolin-induced glucose release in cells transduced with adeno-CA-CaMKII (Figures 2C and S1D). HCs transduced with adeno-KD-CaMKII, which resulted in ~40% decrease in CaMKII activity (Figure S1E), showed decreased forskolin-induced glucose production (Figures 2C).

The role of CaMKII on HGP prompted us to investigate transcriptional effects on two genes encoding enzymes that regulate HGP, glucose-6-phosphatase and phosphoenolpyruvate carboxykinase. To this end, we assayed *G6pc* and *Pck1* mRNA levels in the models described above (Figures 2D–E). In all cases, knockout or KD-CaMKII-mediated inhibition of CaMKII lowered forskolin- or glucagon-induced gene expression, whereas CA-CaMKII increased gene expression. In the absence of forskolin or glucagon, expression levels of *G6pc* and *Pck1* mRNA in WT HCs were much lower than those in hormone-treated WT HCs, but even under these conditions CaMKIIγ deficiency led to a lowering of gene expression (Figure S1F). Moreover, adeno-KD-CaMKII did not decrease the low but detectable level of forskolin-induced *G6pc* mRNA in HCs lacking CaMKIIγ (Figure S1G), consistent with the premise that the suppressive effect of KD-CaMKII on *G6pc* in Fig. 2E is due to CaMKII inhibition. In summary, the CaMKII deficiency and inhibition data show the importance of endogenous CaMKII in glucose production and *Pck1/G6pc* gene expression, while the data with CA-CaMKII show that when the enzyme is expressed at a high level, it can force these processes in the absence of hormones or increase them in the presence of hormones.

Hepatic glucose production *in vivo* is impaired by CaMKIIγ deficiency and stimulated by constitutively active CaMKII

To assess the functional role of CaMKII in hepatic glucose metabolism *in vivo*, we first examined fasting blood glucose levels in WT and *Camk2g*$^{-/-}$ mice. Consistent with our *in vitro* data, we observed a modest but statistically significant decrease in blood glucose levels in fasted *Camk2g*$^{-/-}$ *vs*. WT mice (Figure 3A). The difference in fasting glucose concentration was not associated with an increase in circulating insulin or a decrease in glucagon concentrations in knockout vs. WT mice (Figure S2A**, left**). The mutant mice also showed lower plasma glucose in response to a pyruvate challenge test (Figure 3B). Consistent with the primary HC data, there was a decrease in *G6pc* and *Pck1* mRNA levels in the livers of fasting *Camk2g*$^{-/-}$ mice (Figure 3C). Similar data were obtained in mice treated with glucagon (Figure 3D).

Consistent with these data, treatment of C57BL/6 mice with adeno-KD-CaMKII, which inhibited liver CaMKII activity by ~45% (Figure S2B), decreased fasting blood glucose (Figure 3E). As above, plasma glucagon and insulin were not different between the control and experimental groups (Figure S2A**, right**). In line with blood glucose data, hepatic expression of *G6pc* and *Pck1* mRNA was lower in mice injected with KD-CaMKII (Figure 3F). Because CaMKII inhibition lowers the level the mRNA for the key glycogenolytic enzyme glucose-6-phosphatase, we examined the effect of acute and chronic CaMKII inhibition on liver glycogen content and, as another indicator of glycogen, the percent of periodic acid-Schiff (PAS) -positive cells. The data show that adeno-KD-CaMKII or CaMKII gene targeting increases hepatic glycogen in fasting mice (Figure 3G).

We next examined the effect of constitutively active hepatic CaMKII in mice by treating mice with adeno-CA-CAMKII. The CA-CaMKII group had elevated blood glucose levels after pyruvate challenge, increased liver *G6pc* and *Pck1* mRNA levels, and increased liver glycogen content (Figure S2C–E). CA-CaMKII administration did not alter plasma glucagon or insulin (data not shown). These combined *in vivo* data show that CaMKII affects plasma glucose levels, pyruvate conversion into glucose, and the expression of hepatic glucose metabolism genes.

CaMKII promotes nuclear localization of FoxO1

A major transcription factor involved in HGP is FoxO1, which is regulated primarily by changes in its localization between the cytoplasm and nucleus (Accili and Arden, 2004). We therefore assayed the distribution of GFP-tagged FoxO1 that was transduced into HCs isolated from WT vs. *Camk2g*$^{-/-}$ mice. Under serum-starved conditions, the majority of GFP-FoxO1 was in the nucleus in WT HCs, whereas *Camk2g*$^{-/-}$ HCs displayed primarily cytosolic localization of GFP-FoxO1 (Figure 4A). Moreover, when HCs were transduced with adeno-CA-CaMKII, FoxO1 became predominantly nuclear, while transduction with adeno-KD-CaMKII caused mostly cytoplasmic FoxO1 (Figure 4B). We noted that nuclear FoxO1 was substantial in cultured HCs under the "basal" cell culture conditions used here, and so the fold increase with CA-CaMKII was limited. We therefore lowered basal nuclear FoxO1 using short incubations with insulin, which then revealed a marked increase in nuclear FoxO1 with CA-CaMKII (Figure 4C). Although this experiment was done using a high level of total CaMKII protein expression (see Fig. S1D), a similar experiment using a lower MOI of CA-CaMKII showed an increase in nuclear FoxO1 at a level of total CaMKII protein that was similar to endogenous CaMKII (Figure S3A). To show relevance *in vivo*, we tested the effect of CaMKIIγ deficiency or inhibition in fasting mice. Nuclear FoxO1 in liver was prominent under fasting conditions (Figure 4D**, top blot**), and it was markedly diminished in *Camk2g*$^{-/-}$ mice or mice transduced with adeno-KD-CaMKII (Figure 4D**, middle 2 blots**). Feeding diminished nuclear FoxO1, and nuclear FoxO1 was increased under these conditions by both CA-CaMKII and glucagon (Figure 4D**, bottom blots)**.

cAMP-mediated induction of *G6pc* mRNA in primary hepatocytes is suppressed ≥50% by *Foxo1* shRNA, suggesting an important role for FoxO1 in the endogenous setting (Matsumoto et al., 2007). Consistent with these data, we found that induction of luciferase downstream of the human *G6PC* promoter was blunted when three consensus FoxO-binding sites were mutated (Ayala et al., 1999; von Groote-Bidlingmaier et al., 2003) (Figure S3B). However, this hepatoma cell line—reporter construct experiment does not distinguish between cAMP and dexamethasone effects and may not accurately reflect the endogenous situation. For example, reporter induction here was much less robust than actual *G6pc* mRNA induction in primary hepatocytes (Matsumoto et al., 2007), and the identified promoter element may not be the only site required for regulation. Therefore, rather than pursue this model further as a way to assess the functional importance of FoxO1 in CaMKII-

mediated *G6pc* expression, we instead focused on induction of endogenous *G6pc* in primary hepatocytes and, most importantly, *in vivo*. To begin, we compared the ability of CA-CaMKII to induce *G6pc* in HCs from WT vs. L-Foxo1 KO mice, which lack FoxO1 in liver (Matsumoto et al., 2007). Consistent with previous studies (Puigserver et al., 2003; Matsumoto et al., 2007), forskolin-induced expression of *G6pc* was suppressed in the absence of FoxO1 (Figure 5A**, right graph**). Most importantly, the increase in *G6pc* mRNA expression by CA-CaMKII was markedly blunted by FoxO1 deficiency. In the absence of forskolin, gene expression was much lower as expected (Figure 5A**, left graph**; note Y-axis scale), but even here CA-CaMKII-induced gene expression was almost completely dependent on FoxO1. Finally, we documented that the nuclear localization of two other transcription factors involved in HGP, CREB and Crtc2, were not decreased by CaMKII inhibition of deficiency (Figure S3C–D). These combined data are consistent with a model in which CaMKII promotes FoxO1 nuclear localization, which then leads to induction of *G6pc*.

To further validate the importance of FoxO1 in the impairment of HGP by CaMKII deficiency or inhibition, we transduced HCs from *Camk2g*$^{-/-}$ mice with adenovirus containing a phosphorylation-defective, constitutively nuclear FoxO1 mutant (FoxO1-ADA) (Nakae et al., 2001). We observed that the suppressive effect of CaMKIIγ deficiency on forskolin-induced *G6pc* and *Pck1* mRNA expression was abrogated by transduction with adeno-FoxO1-ADA (Figure 5B). Note that the level of FoxO1-ADA used here was low enough so as not to increase *G6pc* or *Pck1* in forskolin-treated WT HCs, and the level of nuclear FoxO1 in the *Camk2g*$^{-/-}$ + ADA group was similar to the endogenous level in the WT + LacZ group (**inset,** Figure 5B). The *Pck1* results in Fig. 5B, as well as those in Figs. 2–3, are interesting in view of the finding that germline knockdown of FoxO1 does not affect *Pck1* induction (Nakae et al., 2002; Barthel et al., 2001). However, more acute silencing of FoxO1 does suppress *Pck1* (Matsumoto et al., 2007), and so manipulations of CaMKII may be more parallel to that setting. Consistent with the effect of FoxO1-ADA on HGP gene expression, treatment of mice with adeno-FoxO1-ADA adenovirus rescued the impairment of glucose homeostasis in adeno-KD-CaMKII-treated mice (Figure 5C–E). Note that this result cannot be explained by defective transduction with adeno-KD in the ADA group (**inset,** Figure 5E). Taken together, these results are consistent with a model in which CaMKII contributes to HGP through promoting nuclear localization of FoxO1.

The role of non-AKT-phospho-FoxO1 sites and p38 MAP kinase in CaMKIIγ-mediated FoxO1 nuclear localization

Insulin/Akt promotes FoxO1 nuclear exclusion through phosphorylation of T24, S253, and S316 (murine residues) (Brunet et al., 1999). Although CaMKII is a kinase, it could activate a phosphatase and thereby promote nuclear localization of FoxO1 by indirectly decreasing the phosphorylation at these sites. However, we found that phosphorylation at these three sites was not altered in liver from *Camk2g*$^{-/-}$ mice (Figure S4A). FoxO1 acetylation, which can also affect FoxO1 localization and activity in HCs (Accili and Arden, 2004), was also not affected by CaMKII deficiency (Figure S4B).

FoxO1 can also be phosphorylated at other Ser/Thr residues by other kinases, such as p38 MAP kinase (Asada et al., 2007), and these phosphorylation events might promote FoxO1 nuclear localization, not exclusion. To assess the possible role of CaMKII in the phosphorylation of non-Akt sites, we used the model displayed in Figure 4A, i.e., serum-starved WT and *Camk2g*$^{-/-}$ (KO) HCs transduced with GFP-FoxO1, which also carries a FLAG tag. FoxO1 was immunopurified using anti-FLAG, followed by reduction, alkylation, and proteolytic digestion using a triple protease protocol developed by MacCoss *et al.* (MacCoss et al., 2002). Phosphorylated peptides were enriched by TiO_2 chromatography

and then analyzed by LC-MS/MS (Cantin et al., 2007) using MS-based shotgun proteomic methods and label-free quantitation by spectral counting (Cantin et al., 2007). The FoxO1 protein was identified with ~70% sequence coverage, and a total of 57 phosphopeptides for WT and 63 phosphopeptides for KO samples were identified (Tables S1 and S2 at http://fields.scripps.edu/published/foxo1_Tabas_2012/). The peptide false discovery rate (FDR) was less than one percent. Stringent selection criteria were used so that all identified phosphopeptides would have high confidence.

These criteria, with further validation using the phosphopeptide analysis tools Debunker and Ascore (Lu et al., 2007; Beausoleil et al., 2006), enabled the identification of 11 phosphorylation sites: S284, S295, S326, S467, S475, T24, S246, S253, S413, S415 and T553 (see Figure S4C for murine FoxO1 sequence). Figure 6A shows the spectral counts, the Debunker score, and Ascore of each of these 11 FoxO1 phosphopeptides from the KO and WT samples. Most phosphorylation sites are well above the high confidence cut-off values of 0.5 and 12 for Debunker and Ascore, respectively. Five sites with slightly lower values of Debunker or A scores were subjected to manual verification, and their annotated tandem mass spectra are shown in Figures S5D–E for KO peptides 4 and 5 and the aforementioned website for WT peptides 7, 10, and 11. The characteristic b- and/or y-ions for the phospho-sites are all identified. The lower scores are most likely due to the low-abundance fragment ions or lack of neutral losses of phosphoric acid because of the nature of the amino acid sequence for these peptides.

The ratio of spectral KO:WT counts, which was calculated only for peptides with a combined spectral count in KO and WT samples above 10, was used to obtain a measure of the relative expression of identified phosphorylated peptides. By this analysis, only phosphorylation of S295, S467, S475 (peptides 2, 4, and 5) were significantly lower in the KO based on a cut-off value of ≤ 0.5, with the ratio of spectral counts in KO vs. WT of 0.45, 0.38 and 0.5, respectively. Although the peptide containing p-S246 had a combined spectral count of 7, and thus did not reach the pre-specified criterion of >10, it showed a lower trend in the KO vs. WT (2 vs. 5, 0.4). In contrast, S326 (peptide 3) had a ratio of 1.65, indicating upregulation in KO vs. WT.

As an initial test of function for the some of the sites lower in the KO, we used an available plasmid encoding FoxO1 with S-A mutations at seven Ser residues (7A-FoxO1), including Ser295 and 475, as well as Ser246 (Asada et al., 2007). When transfected to a similar levels in *Foxo1*$^{-/-}$ HCs, 7A-FoxO1 showed strikingly less nuclear localization than WT FoxO1 in response to glucagon, while cytoplasmic FoxO1 was higher in the cells transfected with the mutant FoxO1 (Figure 6B). We also tested a construct that had the same seven S-A mutations as in 7A plus 2 additional S-A mutations in S326 and S467 (mutant 9A) (Asada et al., 2007). This mutant showed similarly defective nuclear localization (Figure S4F). Moreover, whereas adeno-CA-CaMKII transduction increased nuclear WT-FoxO1, consistent with the data in Fig. 4D, CA-CaMKII did not increase nuclear 7A-FoxO1 (Figure 6C). These combined data are consistent with a model in which CaMKII directly or indirectly alters the phosphorylation of certain Ser residues in FoxO1 in a manner that promotes its nuclear localization.

Asada et al. (Asada et al., 2007) found evidence of FoxO1 phosphorylation at several sites, including Ser284, 295, 467, and 475, in HEK293T cells transfected with the upstream p38 kinase MKK6. Because p38 has been implicated in the stimulation of HGP (Cao et al., 2005), and CaMKII can activate p38 when studied in neurons (Blanquet, 2000), we considered the possibility of a CaMKII → p38 → FoxO1 phosphorylation/nuclear localization pathway involved in HGP. We first confirmed that p38 was phosphorylated, which is a measure of its activation, in the livers of fasting mice (Figure S5A) and that

inhibition of p38 by the high-affinity competitive inhibitor SB202190 blocked the expression of *G6pc* and *Pck1* in glucagon-stimulated HC (Figure S5B**, left**). The inhibitor data were confirmed using adeno-Cre-transduced HCs isolated from the livers of from *P38a*$^{fl/fl}$ mice (Figure S5B**, right**). To test a potential link between CaMKII and p38, we compared serum-starved HCs from WT and *Camk2g*$^{-/-}$ mice and found a striking decrease in phospho-p38 in the CaMKIIγ-deficient HCs (Figure S5C). We then determined whether p38 was involved in hepatic FoxO1 nuclear localization *in vivo* by comparing fasting mice treated with SB202190 vs. vehicle control. Among the 7 mice in each group, there was a certain degree of variability in both the basal level of p-MK2, a p38 kinase target that reflects p38 activity, and in the level of inhibition of MK2 phosphorylation by SB202190. We therefore plotted nuclear FoxO1 for all 14 mice as a function of p-MK2. The data show a clear decrease in nuclear FoxO1 in mice as a function of p38 inhibition, *i.e.*, as indicated by lower p-MK2 (Figure S5D). Moreover, the p38 inhibitor decreased nuclear GFP-FoxO1 in HCs treated with glucagon (Figure S5E). These combined data are consistent with a model in which CaMKII promotes FoxO1 nuclear localization through p38 activation. Whether p38 functions in CaMKII-induced FoxO1 nuclear localization by directly phosphorylating the aforementioned Ser residues in FoxO1 (Asada et al., 2007) remains to be determined.

The role of CaMKII in hepatic glucose metabolism in obesity

Elevated HGP, in part due to an imbalance of glucagon-to-insulin signaling, contributes to fasting hyperglycemia in obesity and other insulin-resistant states (Sorensen et al., 2006; Unger and Cherrington, 2012; Saltiel, 2001). To test the role of CaMKIIγ in hepatic glucose metabolism in the setting of obesity, we first sought evidence of hepatic CaMKIIγ activation in two mouse models of obesity. We found that the level of p-CaMKII, but not total CaMKII, was markedly higher in the livers of both *ob/ob* mice and WT mice placed on a high-fat, high-calorie diet for 20 wks (diet-induced obesity; DIO) (Figure 7A). Antibody specificity for both anti-p-CaMKII and anti-CaMKII in obese liver is shown by the absence of the immunoblot bands in obese *Camk2g*$^{-/-}$ mice. We next tested functional importance by comparing fasting plasma glucose and hepatic FoxO1-target gene expression in *ob/ob* mice transduced with adeno-KD-CaMKII vs. adeno-LacZ control. The mice treated with adeno-KD-CaMKII had lower fasting glucose, lower blood glucose after pyruvate challenge, and lower expression of three FoxO1-target genes, including *G6pc* and *Pck1* (Figure 7B–D) These changes were not associated with either higher plasma insulin or lower weight in the adeno-KD-CaMKII-treated mice (data not shown). Thus, hepatic CaMKII is activated in the livers of obese mice and regulates hepatic glucose metabolism and FoxO1-target gene expression.

DISCUSSION

The data in this report provide evidence for calcium-mediated regulation of HGP as part of a pathway that can be summarized as follows: glucagon/fasting → cAMP/PKA → IP3R1 → $Ca^{2+}{}_i$ → **CaMKII** → nuclear FoxO1 → HGP. CaMKII also mediates elevated HGP in obese mice (Figure 7), and although more work is needed in this area, it is possible that driving force here is also glucagon (Sorensen et al., 2006; Unger and Cherrington, 2012; Saltiel, 2001). As such, the present findings have implications for three fundamental areas related to HGP: the molecular mechanisms whereby glucagon and fasting, as well as obesity/insulin resistance, stimulate HGP; the molecular links between intracellular calcium and HGP; and the regulation of FoxO1 nuclear transport. The latter issue is of particular interest, because while there have been many reports on how insulin/AKT-mediated phosphorylation of FoxO1, as well as FoxO1 acetylation, promote nuclear exclusion of FoxO1 (Lin and Accili, 2011; van der Horst and Burgering, 2007), there has been little

emphasis on the regulation of FoxO1 nuclear *entry* that occurs in the absence of insulin or in the setting of insulin resistance.

The CaMKII pathway is downstream of cAMP/PKA, and so it would naturally complement other glucagon-PKA pathways that stimulate HGP. Thus far, our data suggest that these other pathways occur in parallel with the CaMKII pathway rather than also being downstream of CaMKII. For example, glucagon-PKA directly phosphorylates cAMP response element binding (CREB) protein, which transcriptionally induces the FoxO1 transcriptional co-factor PGC1α (Herzig et al., 2001), but there was no difference in nuclear CREB in livers from adeno-LacZ vs. KD-CaMKII mice (Figure S3B). This was an important finding, because there are *in vitro* data in neurons and in RANKL-treated RAW264.7 cells that CaMKII can activate/phosphorylate CREB in certain settings (Dash et al., 1991; Sheng et al., 1991; Ang et al., 2007). We also found that CaMKII deficiency did not affect nuclear Crtc2 (Figure S3C), which is another transcriptional activator involved in HGP. These data indicate that CaMKII in liver works in parallel with these other pathways, which together effect the nuclear localization of the proper array of transcriptional factors to mediate HGP. The case with Crtc2 is particularly interesting, because glucagon/PKA-mediated IP3R activation and ER calcium release promotes Crtc2 nuclear localization through another calcium-sensing enzyme, calcineurin (Y. Wang, G. Li, J. Goode, J. C. Paz, R. Screaton, W. H. Fischer, I. Tabas, and M. Montminy, manuscript submitted for publication). Indeed, we found that inhibition of CaMKII and calcineurin are additive in terms of suppressing forskolin-induced *G6pc* mRNA (unpublished data). Thus, a common proximal signaling pathway leads to the coordinated nuclear entry of two key HGP transcription factors, Crtc2 and FoxO1, by different distal mechanisms. In this regard, it is interesting to note a previous study showing that drugs that promote calcium entry through the plasma membrane actually decrease *Pck1* mRNA in HCs (Valera et al., 1993), which may suggest that the route of calcium entry into the cytoplasm is a factor in determining downstream events.

FoxO1 is phosphorylated at Thr24, Ser253, and Ser316 (murine sequence numbers) by insulin/growth factors via Akt to promote its nuclear exclusion. It would be counterintuitive to propose that CaMKII phosphorylates these sites, because CaMKII promotes FoxO1 nuclear localization, but CaMKII could theoretically activate a phosphatase that de-phosphorylates these sites. However, CaMKIIγ deficiency did not affect the phosphorylation of these three residues, and it also did not affect FoxO1 acetylation (Figure S4A–B). Instead, we found evidence that CaMKII mediates the phosphorylation of other Ser residues on FoxO1, and our Ser-Ala FoxO1 mutant experiments suggest that this action plays a role in CaMKII-mediated FoxO1 nuclear localization.

The link between CaMKII and FoxO1 phosphorylation may be direct or indirect. An indirect mechanism, *i.e.*, whereby CaMKII activates another kinase, could be linked to previous findings that other kinases can phosphorylate FoxO on non-Akt sites in a manner that promotes their nuclear retention (Essers et al., 2004; Chiacchiera and Simone, 2010). Based on the p38 inhibitor and gene-targeting data herein and the study of Asada *et al.* (Asada et al., 2007), we suggest that p38 MAPK may also be able to carry out this function and, indeed, may be the mediator of CaMKII-induced FoxO1 nuclear localization. In support of this hypothesis are reports of links between CaMKII and p38 and between p38 and HGP (Cao et al., 2005; Blanquet, 2000). While there is no direct evidence yet that p38 phosphorylates and thereby activates FoxO1, the ability of glucocorticoids to promote FoxO1 nuclear localization in rat cardiomyocytes correlated with activation/phosphorylation of nuclear p38, and immunofluorescence microscopy and IP/immunoblot data suggested that p-P38 and FoxO1 may interact with each other (Puthanveetil et al., 2010). Interestingly, there is evidence that FoxO1 may be able to activate p38 in HCs (Naimi et al., 2007), and so

it is possible that a FoxO1-p38 feed-forward pathway might amplify the effect the CaMKII-p38 pathway suggested here on FoxO1 nuclear localization. However, more work is needed to establish the role of p38 and to further elucidate the mechanisms whereby CaMKII promotes FoxO1 nuclear localization.

The discovery of the role of calcium-CaMKII in HGP not only provides insight into the physiologic defense against fasting hypoglycemia but may also reveal therapeutic targets for the disturbed glucose metabolism that occurs in the setting of insulin resistance, as suggested by the data in Figure 7. Indeed, in type 2 diabetes, disproportionate HGP and an imbalance of glucagon vs. insulin signaling contributes to fasting hyperglycemia (Sorensen et al., 2006; Saltiel, 2001). Moreover, glucagon signaling has also been implicated in type 1 diabetes (Unger and Cherrington, 2012). In this context, future studies will further address the pathophysiologic role(s) and mechanisms of hepatic CaMKIIγ in obesity, insulin resistance, and diabetes and thereby evaluate its potential as a therapeutic target in these disorders.

EXPERIMENTAL PROCEDURES

Measurement of CaMKII Activity

CaMKII activity was assayed using a CaMKII assay kit from Promega according to the manufacturer's instructions. After the HCs were treated as indicated in the figure legends, they were lysed by a 5-min exposure to 1% Triton-X100 in 50 mM HEPES, 150 mM NaCl, 10 mM Na pyrophosphate, 10 mM EDTA, 10 mM EGTA, 1 mM Na_3VO_4, 50 mM NaF, 1 mM PMSF, and 5 μg ml^{-1} leupeptin. Next, [γ-^{32}P]ATP and biotinylated CaMKII peptide substrate were added to the lysate or to the immunoprecipitated complexes (see below). After incubation for 10 min at 30°C, the [^{32}P]-phosphorylated substrate was separated from the residual [^{32}P]ATP using SAM biotin-capture membrane and then quantitated using a scintillation counter. Assays were conducted ± calmodulin, and the activity value in the absence of calmodulin was subtracted from those obtained in the presence of calmodulin.

Glucose Production in Primary HCs

Glucose production assays were carried out as described (Yoon et al., 2001). Briefly, after primary mouse HCs were harvested and cultured as described above, the cell culture medium was switched to glucose- and phenol-free DMEM (pH 7.4) supplemented with 20 mM sodium lactate and 2 mM sodium pyruvate. After 16 h of culture, 500 μl medium was collected, and the glucose content was measured using a colorimetric glucose assay kit (Abcam). The readings were then normalized to the total protein amount in the whole-cell lysates.

Mouse Experiments

Camk2g$^{-/-}$ mice were generated as described previously (Backs et al., 2010) and crossed onto the C57BL6/J background. *ob/ob* mice were obtained from Jackson Labs. Mice were fed a standard chow diet, or a high-fat diet with 60% kcal from fat for the experiments in Fig. 7, and maintained on a 12-h light-dark cycle. Recombinant adenovirus (1.5×10^9 plaque-forming unit/mice) was delivered by tail vein injection, and experiments were commenced after 5 days. Fasting blood glucose was measured in mice that were fasted for 12–14 h, with free access to water, using a glucose meter (One Touch Ultra, Lifescan). Pyruvate-tolerance tests were carried out with an intraperitoneal injection of 2 g kg^{-1} body weight pyruvate after 17 h of fasting. Blood glucose levels were measured over the following 2 h. Xestospongin C was administered by daily i.p. injections to mice at a dose of 10 pmol g^{-1} for 4 days. *P38a*$^{fl/fl}$ mice were generated as described previously (Engel et al., 2005) and generously provided by Dr. Yibin Wang, UCLA School of Medicine.

Hepatic Glycogen Measurement

50 –100 mg of frozen livers were homogenized in 1 ml of H_2O with protease and phosphatase inhibitors. Samples were then mixed with KOH (1:2), boiled for 25 min and washed with 70% ethanol. The pellet was dried and dissolved in 100 μl H_2O, and the glycogen content was assessed using the Glycogen Assay Kit (Abcam) according to the manufacturer's instructions. Data represent the mean ± SEM.

PAS Staining of Mouse Liver Sections

Liver samples were fixed in 10% neutral-buffered formalin for 24 h and embedded in paraffin. Sections (5 micron) were stained for glycogen using Periodic acid-Schiff (PAS) stain (Sigma) according to manufacturer's instructions. The sections were then counterstained with hematoxylin and examined by light microscopy. For the quantification of PAS staining, 5 fields from 4 different sections were chosen randomly, and the number of PAS-positive cells was counted and expressed as the percentage of the total number of cells (Hammad et al., 1982). Two independent investigators, blinded to the identity of the samples, performed the analysis.

Analysis of Mass Spectrometric Data

Protein and phosphopeptide identification, quantification, and phospho analysis were performed with Integrated Proteomics Pipeline - IP2 (Integrated Proteomics Applications, Inc., San Diego, CA. http://www.integratedproteomics.com/) using ProLuCID, DTASelect2, Census, DeBunker and Ascore. Spectrum raw files were extracted into ms1 and ms2 files (McDonald et al., 2004) from raw files using RawExtract 1.9.9 (http://fields.scripps.edu/downloads.php), and the tandem mass spectra were searched against EBI IPI mouse protein database (http://www.ebi.ac.uk/IPI/IPImouse.html, released on March 24, 2010). In order to accurately estimate peptide probabilities and false discovery rates, we used a decoy database containing the reversed sequences of all the proteins appended to the target database (Peng et al., 2003). Tandem mass spectra were matched to sequences using the ProLuCID (Xu et al., 2006) algorithm with 50 ppm peptide mass tolerance. ProLuCID searches were done on an Intel Xeon cluster running under the Linux operating system. The search space included all fully- and half-tryptic peptide candidates that fell within the mass tolerance window. Carbamidomethylation (+57.02146 Da) of cysteine was considered as a static modification, while phosphorylation (+79.9663) on serine, threonine, and tyrosine were considered as variable modifications.

The validity of peptide/spectrum matches (PSMs) was assessed in DTASelect (Tabb et al., 2002; Cociorva et al., 2007) using two SEQUEST (Eng et al., 1994) defined parameters, the cross-correlation score (XCorr), and normalized difference in cross-correlation scores (DeltaCN). The search results were grouped by charge state (+1, +2, +3, and greater than +3) and tryptic status (fully tryptic, half-tryptic, and non-tryptic), resulting in 12 distinct sub-groups. In each one of these sub-groups, the distribution of Xcorr, DeltaCN, and DeltaMass values for (a) direct and (b) decoy database PSMs was obtained, and then the direct and decoy subsets were separated by discriminant analysis. Full separation of the direct and decoy PSM subsets is not generally possible; therefore, peptide match probabilities were calculated based on a nonparametric fit of the direct and decoy score distributions. A peptide confidence of 99.5% was set as the minimum threshold, and only phosphopeptides with delta mass less than 10 ppm were accepted. The false discovery rate was calculated as the percentage of reverse decoy PSMs among all the PSMs that passed the 99.5% confidence threshold. After this last filtering step, we estimate that both the protein and peptide false discovery rates were both below 0.1%. After database searching and DTASelect2 filtering, phosphopeptides were analyzed with IP2 phospho analysis tool that

uses Ascore (Beausoleil et al., 2006) and Debunker (Lu et al., 2007). Peptides and phosphopeptides were quantified using the Spectral Count method (Liu et al., 2004).

Statistical Analysis

All results are presented as mean ± SEM. P values were calculated using the student's t-test for normally distributed data and the Mann-Whitney rank sum test for non-normally distributed data.

HIGHLIGHTS

- Fasting and glucagon activate hepatic CaMKII in a PKA-IP3R1-Ca^{2+}_i-dependent manner
- CaMKII promotes fasting/glucagon-induced hepatic glucose production (HGP)
- CaMKII promotes nuclear FoxO1, which is required for CaMKII-mediated stimulation of HGP
- The CaMKII-FoxO1 pathway is also involved in excessive HGP in the setting of obesity.

Supplementary Material

Refer to Web version on PubMed Central for supplementary material.

Acknowledgments

We thank Dr. Eric Olson (University of Texas Southwestern Medical Center) for the *Camk2g*$^{-/-}$ mice and Dr. Marc Montminy (Salk Institute for Biological Sciences) for anti-Crtc2 antibody. This work was supported by an American Heart Association Scientist Development Grant to L. Ozcan; Emmy Noether-DFG grant 2258/2-1 to J. Backs; and NIH grants P41 RR011823 to C.C.L. Wong and J. Yates III, NHLBI Proteomic Centers grant HHSN268201000035C to T. Xu, HL49426 to H.A. Singer, HL087123 and DK057539 to D. Accili, and HL087123 and HL075662 to I. Tabas.

REFERENCES

Accili D, Arden KC. FoxOs at the crossroads of cellular metabolism, differentiation, and transformation. Cell. 2004; 117:421–426. [PubMed: 15137936]

Ang ES, Zhang P, Steer JH, Tan JW, Yip K, Zheng MH, Joyce DA, Xu J. Calcium/calmodulin-dependent kinase activity is required for efficient induction of osteoclast differentiation and bone resorption by receptor activator of nuclear factor kappa B ligand (RANKL). J. Cell Physiol. 2007; 212:787–795. [PubMed: 17477372]

Asada S, Daitoku H, Matsuzaki H, Saito T, Sudo T, Mukai H, Iwashita S, Kako K, Kishi T, Kasuya Y, Fukamizu A. Mitogen-activated protein kinases, Erk and p38, phosphorylate and regulate Foxo1. Cell Signal. 2007; 19:519–527. [PubMed: 17113751]

Ayala JE, Streeper RS, Desgrosellier JS, Durham SK, Suwanichkul A, Svitek CA, Goldman JK, Barr FG, Powell DR, O'Brien RM. Conservation of an insulin response unit between mouse and human glucose-6-phosphatase catalytic subunit gene promoters: transcription factor FKHR binds the insulin response sequence. Diabetes. 1999; 48:1885–1889. [PubMed: 10480625]

Backs J, Stein P, Backs T, Duncan FE, Grueter CE, McAnally J, Qi X, Schultz RM, Olson EN. The gamma isoform of CaM kinase II controls mouse egg activation by regulating cell cycle resumption. Proc. Natl. Acad. Sci. U. S. A. 2010; 107:81–86. [PubMed: 19966304]

Barthel A, Schmoll D, Kruger KD, Bahrenberg G, Walther R, Roth RA, Joost HG. Differential regulation of endogenous glucose-6-phosphatase and phosphoenolpyruvate carboxykinase gene expression by the forkhead transcription factor FKHR in H4IIE-hepatoma cells. Biochem. Biophys. Res. Commun. 2001; 285:897–902. [PubMed: 11467835]

Beausoleil SA, Villen J, Gerber SA, Rush J, Gygi SP. A probability-based approach for high-throughput protein phosphorylation analysis and site localization. Nat. Biotechnol. 2006; 24:1285–1292. [PubMed: 16964243]

Blanquet PR. Identification of two persistently activated neurotrophin-regulated pathways in rat hippocampus. Neuroscience. 2000; 95:705–719. [PubMed: 10670437]

Brunet A, Bonni A, Zigmond MJ, Lin MZ, Juo P, Hu LS, Anderson MJ, Arden KC, Blenis J, Greenberg ME. Akt promotes cell survival by phosphorylating and inhibiting a Forkhead transcription factor. Cell. 1999; %19;96:857–868.

Burgess SC, He T, Yan Z, Lindner J, Sherry AD, Malloy CR, Browning JD, Magnuson MA. Cytosolic phosphoenolpyruvate carboxykinase does not solely control the rate of hepatic gluconeogenesis in the intact mouse liver. Cell Metab. 2007; 5:313–320. [PubMed: 17403375]

Bygrave FL, Benedetti A. Calcium: its modulation in liver by cross-talk between the actions of glucagon and calcium-mobilizing agonists. Biochem. J. 1993; 296:1–14. [PubMed: 8250828]

Cantin GT, Shock TR, Park SK, Madhani HD, Yates JR III. Optimizing TiO2-based phosphopeptide enrichment for automated multidimensional liquid chromatography coupled to tandem mass spectrometry. Anal. Chem. 2007; 79:4666–4673. [PubMed: 17523591]

Cao W, Collins QF, Becker TC, Robidoux J, Lupo EG Jr, Xiong Y, Daniel KW, Floering L, Collins S. p38 Mitogen-activated protein kinase plays a stimulatory role in hepatic gluconeogenesis. J. Biol Chem. 2005; 280:42731–42737. [PubMed: 16272151]

Chiacchiera F, Simone C. The AMPK-FoxO3A axis as a target for cancer treatment. Cell Cycle. 2010; 9:1091–1096. [PubMed: 20190568]

Cociorva D, Tabb L, Yates JR. Chapter 13 Validation of tandem mass spectrometry database search results using DTASelect. Curr. Protoc. Bioinformatics. 2007; (Unit 13.4) Unit.

Couchonnal LF, Anderson ME. The role of calmodulin kinase II in myocardial physiology and disease. Physiology. (Bethesda.). 2008; 23:151–159. [PubMed: 18556468]

Dash PK, Karl KA, Colicos MA, Prywes R, Kandel ER. cAMP response element-binding protein is activated by Ca2+/calmodulin- as well as cAMP-dependent protein kinase. Proc Natl Acad Sci U S A. 1991; 88:5061–5065. [PubMed: 1647024]

Eng JK, McCormack AL, Yates JR III. An approach to correlate tandem mass spectral data of peptides with amino acid sequences in a protein database. J. Am. Soc. Mass Spectrometry. 1994; 5:976–989.

Engel FB, Schebesta M, Duong MT, Lu G, Ren S, Madwed JB, Jiang H, Wang Y, Keating MT. p38 MAP kinase inhibition enables proliferation of adult mammalian cardiomyocytes. Genes Dev. 2005; 19:1175–1187. [PubMed: 15870258]

Essers MA, Weijzen S, de Vries-Smits AM, Saarloos I, de Ruiter ND, Bos JL, Burgering BM. FOXO transcription factor activation by oxidative stress mediated by the small GTPase Ral and JNK. EMBO J. 2004; 23:4802–4812. [PubMed: 15538382]

Friedmann N, Rasmussen H. Calcium, manganese and hepatic gluconeogenesis. Biochim. Biophys. Acta. 1970; 222:41–52. [PubMed: 4319790]

Hall RK, Sladek FM, Granner DK. The orphan receptors COUP-TF and HNF-4 serve as accessory factors required for induction of phosphoenolpyruvate carboxykinase gene transcription by glucocorticoids. Proc Natl Acad Sci U S A. 1995; 92:412–416. [PubMed: 7831301]

Hammad ES, Striffler JS, Cardell RR Jr. Morphological and biochemical observations on hepatic glycogen metabolism in genetically diabetic (db/db) mice. Diabete Metab. 1982; 8:147–153. [PubMed: 7049780]

Hansen LH, Gromada J, Bouchelouche P, Whitmore T, Jelinek L, Kindsvogel W, Nishimura E. Glucagon-mediated Ca2+ signaling in BHK cells expressing cloned human glucagon receptors. Am. J. Physiol. 1998; 274:C1552–C1562. [PubMed: 9611120]

Harano Y, Kashiwagi A, Kojima H, Suzuki M, Hashimoto T, Shigeta Y. Phosphorylation of carnitine palmitoyltransferase and activation by glucagon in isolated rat hepatocytes. FEBS Lett. 1985; 188:267–272. [PubMed: 2411597]

Herzig S, Long F, Jhala US, Hedrick S, Quinn R, Bauer A, Rudolph D, Schutz G, Yoon C, Puigserver P, Spiegelman B, Montminy M. CREB regulates hepatic gluconeogenesis through the coactivator PGC-1. Nature. 2001; 413:179–183. [PubMed: 11557984]

Kraus-Friedmann N, Feng L. The role of intracellular Ca2+ in the regulation of gluconeogenesis. Metabolism. 1996; 45:389–403. [PubMed: 8606649]

Lin HV, Accili D. Hormonal regulation of hepatic glucose production in health and disease. Cell Metab. 2011; 14:9–19. [PubMed: 21723500]

Liu H, Sadygov RG, Yates JR III. A model for random sampling and estimation of relative protein abundance in shotgun proteomics. Anal. Chem. 2004; 76:4193–4201. [PubMed: 15253663]

Lu B, Ruse C, Xu T, Park SK, Yates J III. Automatic validation of phosphopeptide identifications from tandem mass spectra. Anal. Chem. 2007; 79:1301–1310. [PubMed: 17297928]

MacCoss MJ, McDonald WH, Saraf A, Sadygov R, Clark JM, Tasto JJ, Gould KL, Wolters D, Washburn M, Weiss A, Clark JI, Yates JR III. Shotgun identification of protein modifications from protein complexes and lens tissue. Proc Natl Acad Sci U S A. 2002; 99:7900–7905. [PubMed: 12060738]

Marques-da-Silva AC, D'Avila RB, Ferrari AG, Kelmer-Bracht AM, Constantin J, Yamamoto NS, Bracht A. Ca2+ dependence of gluconeogenesis stimulation by glucagon at different cytosolic NAD(+)-NADH redox potentials. Braz. J. Med. Biol Res. 1997; 30:827–836. [PubMed: 9361705]

Matsumoto M, Pocai A, Rossetti L, Depinho RA, Accili D. Impaired regulation of hepatic glucose production in mice lacking the forkhead transcription factor Foxo1 in liver. Cell Metab. 2007; 6:208–216. [PubMed: 17767907]

McDonald WH, Tabb DL, Sadygov RG, MacCoss MJ, Venable J, Graumann J, Johnson JR, Cociorva D, Yates JR III. MS1, MS2, and SQT-three unified, compact, and easily parsed file formats for the storage of shotgun proteomic spectra and identifications. Rapid Commun. Mass Spectrom. 2004; 18:2162–2168. [PubMed: 15317041]

Mine T, Kojima I, Ogata E. Role of calcium fluxes in the action of glucagon on glucose metabolism in rat hepatocytes. Am. J. Physiol. 1993; 265:G35–G42. [PubMed: 8393298]

Naimi M, Gautier N, Chaussade C, Valverde AM, Accili D, Van OE. Nuclear forkhead box O1 controls and integrates key signaling pathways in hepatocytes. Endocrinology. 2007; 148:2424–2434. [PubMed: 17303659]

Nakae J, Biggs WH III, Kitamura T, Cavenee WK, Wright CV, Arden KC, Accili D. Regulation of insulin action and pancreatic beta-cell function by mutated alleles of the gene encoding forkhead transcription factor Foxo1. Nat. Genet. 2002; 32:245–253. [PubMed: 12219087]

Nakae J, Kitamura T, Silver DL, Accili D. The forkhead transcription factor Foxo1 (Fkhr) confers insulin sensitivity onto glucose-6-phosphatase expression. J. Clin. Invest. 2001; 108:1359–1367. [PubMed: 11696581]

Peng J, Elias JE, Thoreen CC, Licklider LJ, Gygi SP. Evaluation of multidimensional chromatography coupled with tandem mass spectrometry (LC/LC-MS/MS) for large-scale protein analysis: the yeast proteome. J. Proteome. Res. 2003; 2:43–50. [PubMed: 12643542]

Pfleiderer PJ, Lu KK, Crow MT, Keller RS, Singer HA. Modulation of vascular smooth muscle cell migration by calcium/ calmodulin-dependent protein kinase II-delta 2. Am J Physiol Cell Physiol. 2004; 286:C1238–C1245. [PubMed: 14761894]

Pilkis SJ, Granner DK. Molecular physiology of the regulation of hepatic gluconeogenesis and glycolysis. Annu. Rev. Physiol. 1992; 54:885–909. 885–909. [PubMed: 1562196]

Puigserver P, Rhee J, Donovan J, Walkey CJ, Yoon JC, Oriente F, Kitamura Y, Altomonte J, Dong H, Accili D, Spiegelman BM. Insulin-regulated hepatic gluconeogenesis through FOXO1-PGC-1alpha interaction. Nature. 2003; 423:550–555. [PubMed: 12754525]

Puthanveetil P, Wang Y, Wang F, Kim MS, Abrahani A, Rodrigues B. The increase in cardiac pyruvate dehydrogenase kinase-4 after short-term dexamethasone is controlled by an Akt-p38-forkhead box other factor-1 signaling axis. Endocrinology. 2010; 151:2306–2318. [PubMed: 20181797]

Radziuk J, Pye S. Hepatic glucose uptake, gluconeogenesis and the regulation of glycogen synthesis. Diabetes Metab Res. Rev. 2001; 17:250–272. [PubMed: 11544610]

Rhee J, Inoue Y, Yoon JC, Puigserver P, Fan M, Gonzalez FJ, Spiegelman BM. Regulation of hepatic fasting response by PPARgamma coactivator-1alpha (PGC-1): requirement for hepatocyte nuclear factor 4alpha in gluconeogenesis. Proc Natl Acad Sci U S A. 2003; 100:4012–4017. [PubMed: 12651943]

Saltiel AR. New perspectives into the molecular pathogenesis and treatment of type 2 diabetes. Cell. 2001; 104:517–529. [PubMed: 11239409]

Sheng M, Thompson MA, Greenberg ME. CREB: a Ca(2+)-regulated transcription factor phosphorylated by calmodulin-dependent kinases. Science. 1991; 252:1427–1430. [PubMed: 1646483]

Singer HA. Ca2+/calmodulin-dependent protein kinase II Function in Vascular Remodeling. J. Physiol. 2011

Sorensen H, Brand CL, Neschen S, Holst JJ, Fosgerau K, Nishimura E, Shulman GI. Immunoneutralization of endogenous glucagon reduces hepatic glucose output and improves long-term glycemic control in diabetic ob/ob mice. Diabetes. 2006; 55:2843–2848. [PubMed: 17003351]

Staddon JM, Hansford RG. Evidence indicating that the glucagon-induced increase in cytoplasmic free Ca2+ concentration in hepatocytes is mediated by an increase in cyclic AMP concentration. Eur. J. Biochem. 1989; 179:47–52. [PubMed: 2537201]

Tabb DL, McDonald WH, Yates JR III. DTASelect and Contrast: tools for assembling and comparing protein identifications from shotgun proteomics. J. Proteome. Res. 2002; 1:21–26. [PubMed: 12643522]

Unger RH, Cherrington AD. Glucagonocentric restructuring of diabetes: a pathophysiologic and therapeutic makeover. J. Clin. Invest. 2012; 122:4–12. [PubMed: 22214853]

Valera A, Solanes G, Bosch F. Calcium-mobilizing effectors inhibit P-enolpyruvate carboxykinase gene expression in cultured rat hepatocytes. FEBS Lett. 1993; 333:319–324. [PubMed: 8224202]

van der Horst A, Burgering BM. Stressing the role of FoxO proteins in lifespan and disease. Nat. Rev. Mol. Cell Biol. 2007; 8:440–450. [PubMed: 17522590]

von Groote-Bidlingmaier F, Schmoll D, Orth HM, Joost HG, Becker W, Barthel A. DYRK1 is a co-activator of FKHR (FOXO1a)-dependent glucose-6-phosphatase gene expression. Biochem. Biophys. Res. Commun. 2003; 300:764–769. [PubMed: 12507516]

Xu T, Venable JD, Park SK, Cociorva D, Lu B, Liao L, Wohlschlegel J, Hewel J, Yates JR. ProLuCID, a fast and senstive tandem mass spectra-based protein identification program. Mol. Cell Proteomics. 2006; 5:S174.

Yoon JC, Puigserver P, Chen G, Donovan J, Wu Z, Rhee J, Adelmant G, Stafford J, Kahn CR, Granner DK, Newgard CB, Spiegelman BM. Control of hepatic gluconeogenesis through the transcriptional coactivator PGC-1. Nature. 2001; 413:131–138. [PubMed: 11557972]

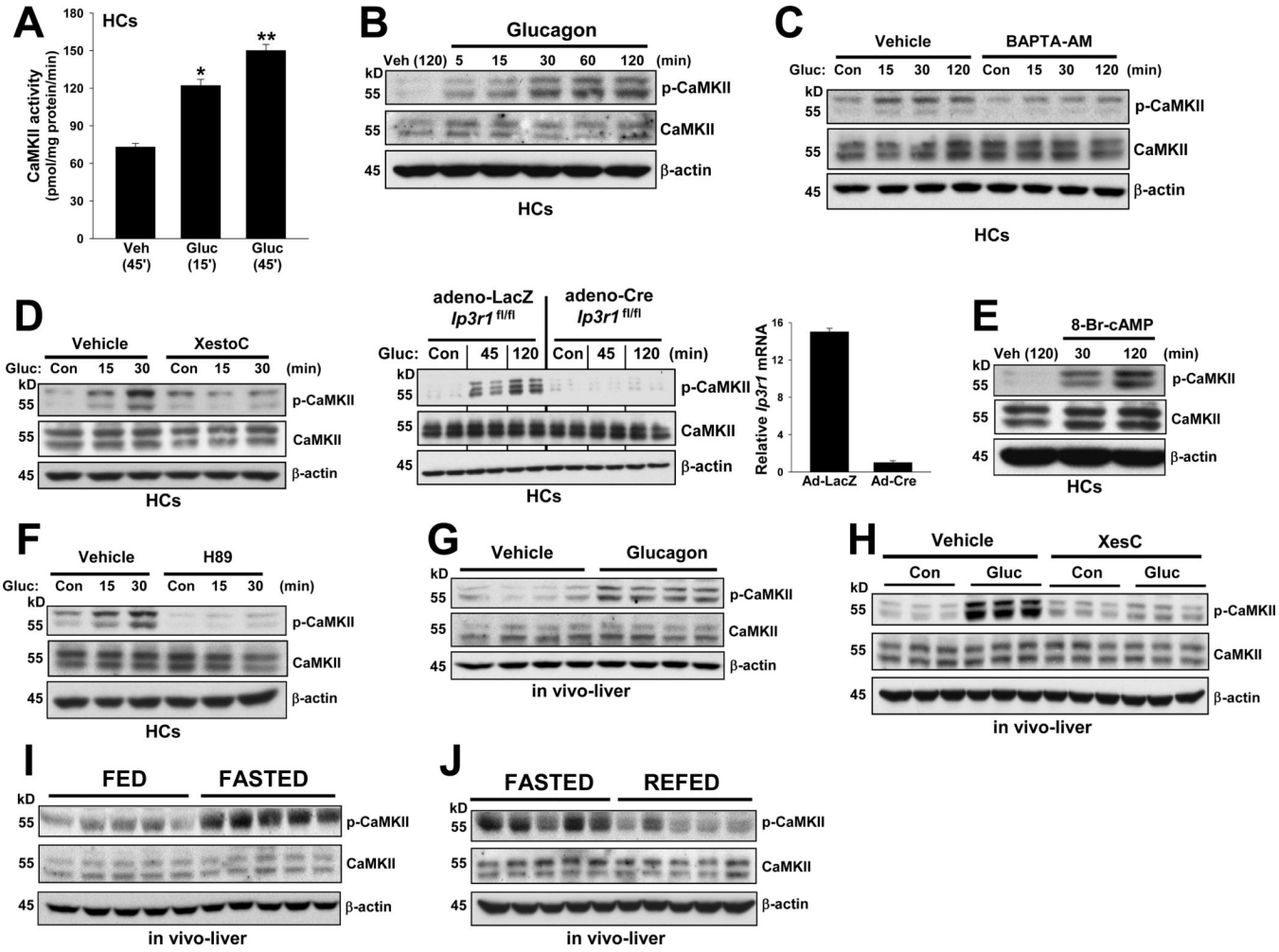

Figure 1. Glucagon and fasting activates hepatic CaMKII

(**A**) CaMKII enzyme activity was assayed in triplicate wells of primary mouse HCs stimulated with 100 nM glucagon (Gluc) or vehicle control (Veh) for the indicated times (*P < 0.05 and **P < 0.01 vs. Veh; mean ± S.E.M.). (**B–J**) Extracts of HCs or liver were probed for phospho-CaMKII, total CaMKII, and β-actin by immunoblot assay. (**B**) HCs were incubated with 100 nM glucagon for the indicated times; (**C**) Glucagon was added to HCs that were pre-treated for 1 h with vehicle control (Veh) or 5 μM BAPTA-AM; (**D**) Glucagon was added to HCs that were pre-treated with 0.5 μM xestospongin (XesC) or to HCs from *Ip3r1*$^{fl/fl}$ mice transduced with adeno-LacZ control or adeno-Cre (bar graph = *Ip3r1* mRNA levels); (**E**) Glucagon was added to HCs that were pre-treated for 1 h with vehicle control (Veh) or 10 μM H89. (**F**) HCs were incubated with 100 μM 8-bromo-cAMP for the indicated times. (**G–J**) *In vivo* experiments. In **G**, mice were treated for 30 min with 200 μg kg^{-1} body weight of glucagon i.p., and in **H**, mice were pre-treated with 10 pmol g^{-1} xestospongin C or vehicle control i.p. 4 days prior to glucagon treatment. In **I–J**, mice were fed ad libitum or fasted for 12 h, or fasted for 12 h and then re-fed for 4 h.

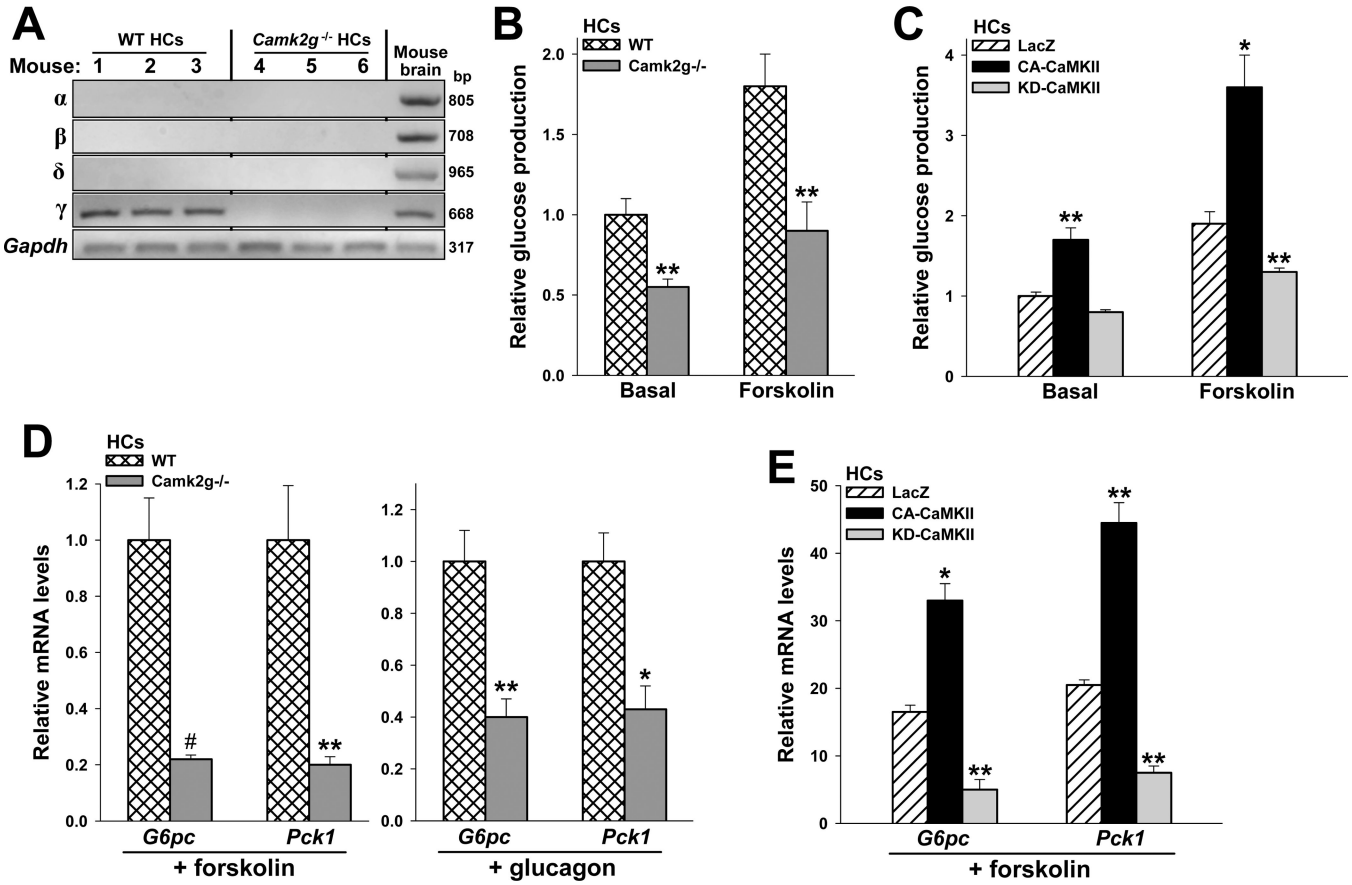

Figure 2. CaMKII regulates glucose production and hepatic *G6Pc* and *Pck1* expression in primary HCs

(**A**) RNA from HCs from 3 WT and 3 *Camk2g*$^{-/-}$ mice and mouse brain from a WT mouse were probed for the indicated *Camk2* isoform mRNAs by RT-PCR. (**B**) HCs from WT and *Camk2g*$^{-/-}$ mice were serum-depleted overnight and then incubated with forskolin (10 μm) for 14 h in serum- and glucose-free media, and then glucose in the medium was assayed (**P < 0.01 vs. WT in each group; mean ± S.E.M.). (**C**) HCs from WT mice were transduced with adenoviral vectors expressing LacZ, CA-CaMKII, or KD-CaMKII at an MOI of 20 and then assayed for glucose production as in (B) (*P < 0.05 and **P < 0.01 vs. LacZ in each group; mean ± S.E.M.). (**D–E**) HCs similar to those in (B) and (C) were serum-depleted overnight and then incubated for 5 h with 10 μM forskolin or 100 nM glucagon in serum-free media, as indicated. RNA was assayed for *G6pc* and *Pck1* mRNA by RT-qPCR (*P < 0.05 and **P < 0.01 vs. LacZ or WT in each group; mean ± S.E.M.).

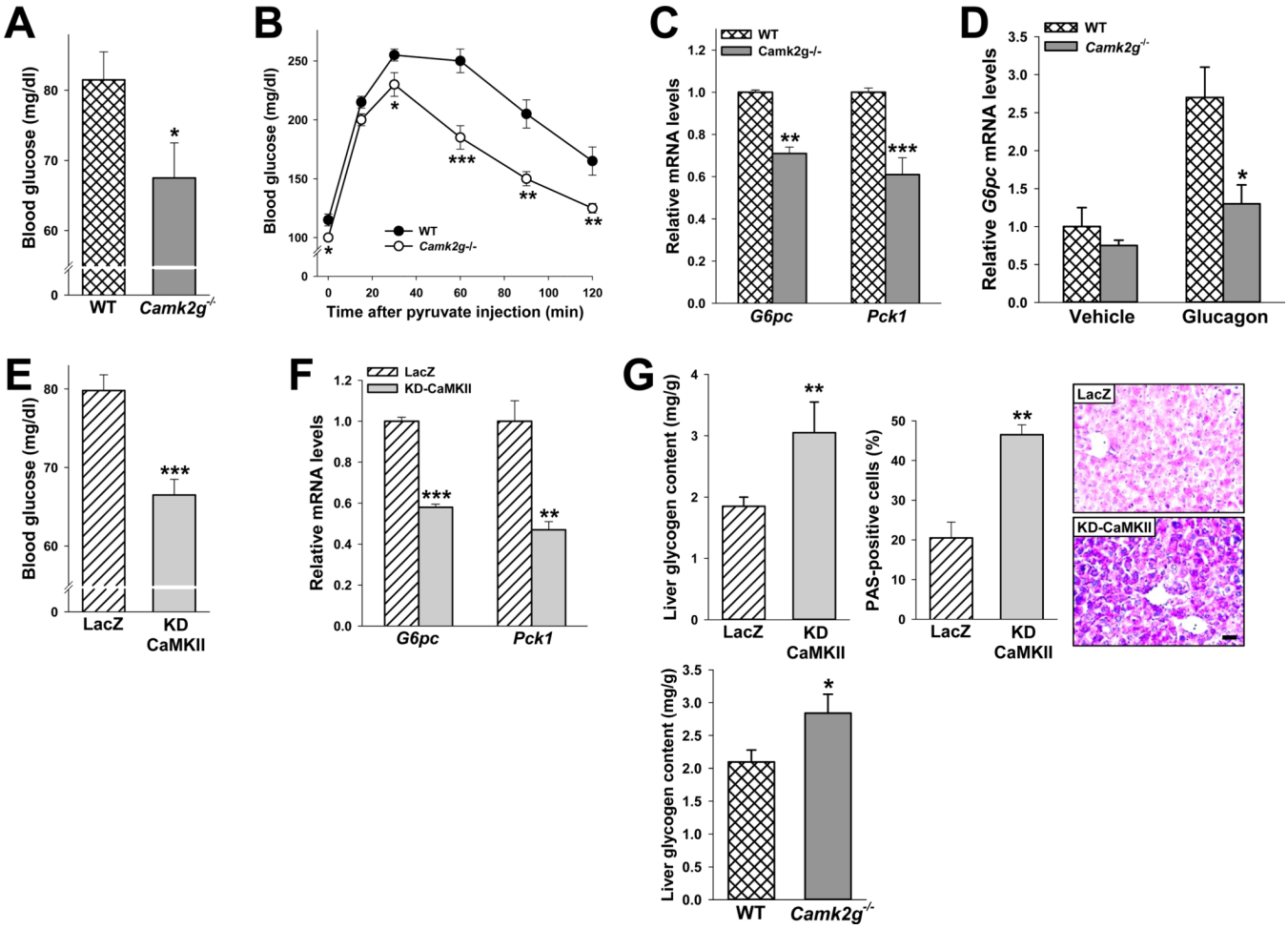

Figure 3. CaMKIIγ deficiency or acute inhibition *in vivo* decreases blood glucose and hepatic *G6pc* and *Pck1*

(**A**) Blood glucose of 12-h-fasted 8-wk/o WT and *Camk2g*$^{-/-}$ mice (*P < 0.05). (**B**) As in (A), but the mice were fasted for 18 h and then challenged with 2 mg kg^{-1} pyruvate (B) (*P < 0.05; **P < 0.01; ***P < 0.005; mean ± S.E.M.). (**C**) Liver *G6pc* and *Pck1* mRNA in 12-h-fasted WT and *Camk2g*$^{-/-}$ mice (**P < 0.01; ***P < 0.001; mean ± S.E.M.). (**D**) WT and *Camk2g*$^{-/-}$ mice were injected i.p. with glucagon (200 μg kg^{-1}) and sacrificed 30 min later. Liver *G6pc* mRNA was assayed (*P < 0.05; mean ± S.E.M.). (**E–G**) 9-wk/o WT mice were administered 1.5 × 10^{9} pfu of adeno-LacZ or KD-CaMKII, and 5 days later the following parameters were assayed in 12-h-fasted mice: **E**, blood glucose (***P < 0.001; mean ± S.E.M.); **F**, liver *G6pc* and *Pck1* mRNA (**P < 0.01; ***P < 0.001; mean ± S.E.M.); and **G**, liver glycogen content and PAS-positive cells (**P < 0.01; mean ± S.E.M.). Panel G also shows liver glycogen content in fasted WT and *Camk2g*$^{-/-}$ mice (*P < 0.05; mean ± S.E.M.). For all panels, n = 5/group except panel D, where n = 4/group.

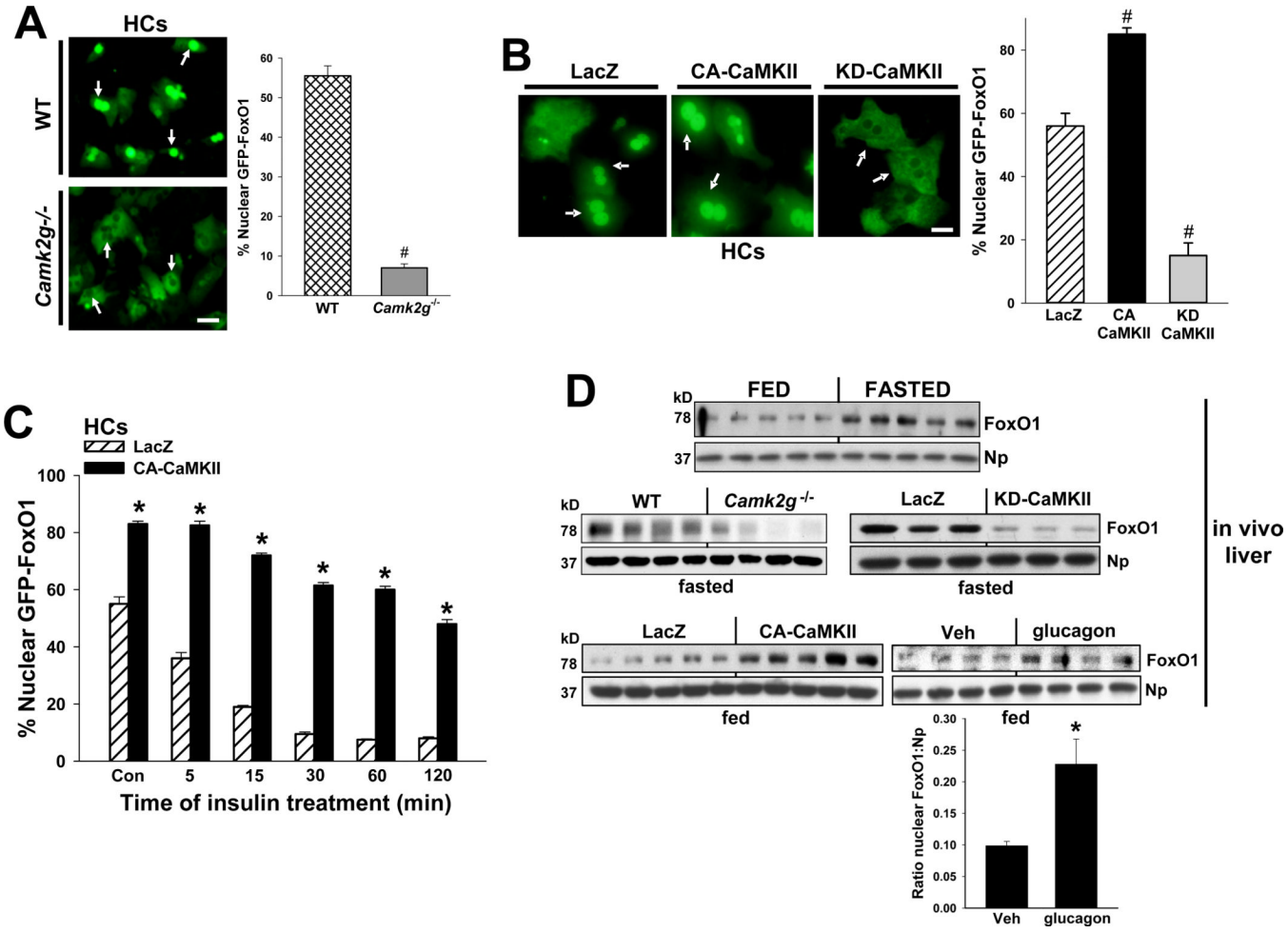

Figure 4. CaMKII regulates hepatic FoxO1 subcellular localization

(**A**) HCs from WT and *Camk2g*$^{-/-}$ mice were transduced with an adenovirus expressing murine GFP-FoxO1 at an MOI of 2. Cells were serum-depleted overnight and then incubated for 5 h in serum-free media. FoxO1 subcellular localization was assessed by indirect immunofluorescence. Bar, 10 μm. Data are quantified in the right panel. ($^{\#}P < 0.0005$; mean ± S.E.M.). (**B**) HCs were transduced with adenoviral vectors expressing LacZ, CA-CaMKII, or KD-CaMKII at an MOI of 20 and then transduced 4 h later with adeno-GFP-FoxO1, followed by fluorescence microscopy and quantification as in (A) ($^{\#}P < 0.005$ vs. LacZ; mean ± S.E.M.). Bar, 5 μm. (**C**) HCs were transduced with adeno-LacZ or CA-CaMKII and then adeno-GFP-FoxO1 as in (B). After incubation in serum-depleted medium o.n. and then serum-free medium for 5 h, the cells were treated with 100 nM insulin for the indicated times. FoxO1 subcellular localization was quantified as in (B) (*P < 0.005 vs. LacZ in each group; mean ± S.E.M.). (**D**) Nuclear FoxO1 and nucleophosmin were probed by immunoblot in livers from fasted WT mice, *Camk2g*$^{-/-}$ mice, or WT mice treated with adeno-LacZ or KD-CaMKII; from fed WT mice treated with adeno-LacZ or CA-CaMKII; or from fed WT mice treated for 30 min with 200 μg kg-1 body weight of glucagon i.p. For the glucagon experiment, the average FoxO:Np densitometric ratio values are in the graph (*P = 0.029; blemishes in lanes 6 and 8 were excluded from the densitometry analysis).

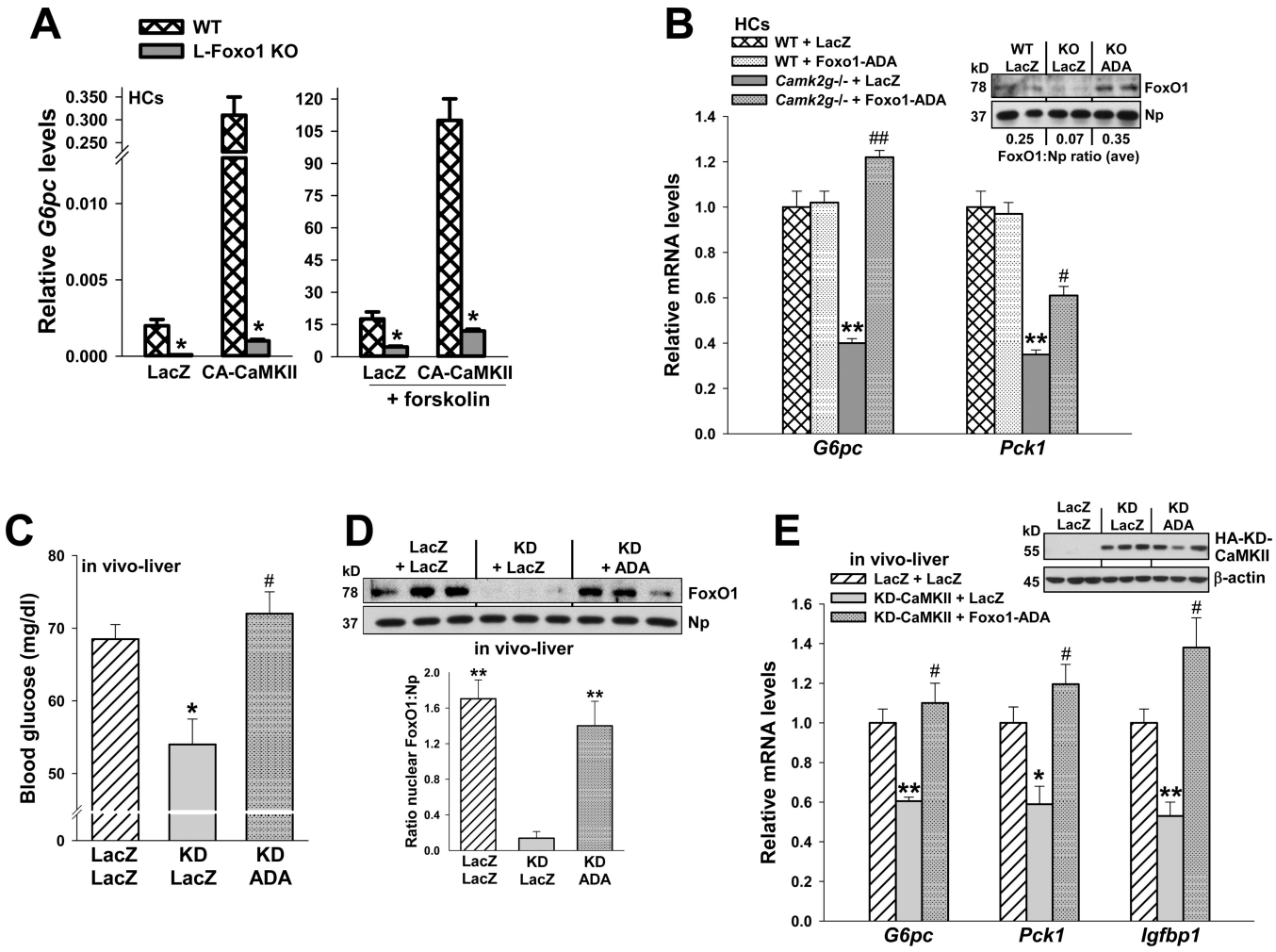

Figure 5. Impairment of glucose metabolism by CaMKII inhibition is rescued by transduction with constitutively nuclear FoxO1-ADA

(**A**) HCs from wild-type or L-FoxO1 knockout mice were transduced with adeno-LacZ or CA-CaMKII. The cells were serum-depleted overnight and then incubated for 5 h in the absence or presence of forskolin (10 μm) in serum-free media. RNA was assayed for *G6pc* mRNA (*P < 0.001; mean ± S.E.M.). (**B**) HCs from WT and *Camk2g*$^{-/-}$ mice were administered adeno-LacZ or FoxO1-ADA at an MOI of 0.2. Cells were serum-depleted overnight and then incubated for 5 h with 10 μM forskolin in serum-free media. RNA was assayed for *G6pc* and *Pck1* mRNA (**P < 0.01 vs. WT groups; $^{\#}$P < 0.05 and $^{\#\#}$P < 0.01 vs. *Camk2g*$^{-/-}$/LacZ group; mean ± S.E.M.). **Inset**, the nuclei from a parallel set of cells were probed for FoxO1 and nucleophosmin by immunoblot; the average densitometric ratio appears below each pair of lanes. (**C–E**) 8-wk/o WT mice were administered adeno-LacZ or KD-CaMKII, and then one day later, half of the adeno-KD-CaMKII mice received adeno-FoxO1-ADA, while the other half received adeno-LacZ control. Blood glucose levels were assayed at day 5 after a 12-h fast (*P < 0.05 vs. LacZ/LacZ; $^{\#}$P < 0.05 vs. KD/LacZ; n = 5/group; mean ± S.E.M.), and liver was assayed for nuclear FoxO1 protein (**P < 0.01 vs. KD/LacZ; mean ± S.E.M.); *G6pc*, *Pck1* and *Igfbp1* mRNA (*P < 0.05 and **P < 0.01 vs. LacZ/LacZ; $^{\#}$P < 0.05 vs. KD/LacZ; n = 3/group; mean ± S.E.M.). The **inset** to panel E shows the level of hemagglutinin (HA)-tagged KD-CaMKII protein (anti-HA immunoblot).

A

Peptide*	Site	Spectral Count # (KO)	Debunker Score (KO)	A Score (KO)	Spectral Count # (WT)	Debunker Score (WT)	A Score (WT)	Spectral Count # Ratio (KO/WT)
1: K.KASLQSGQEGPGDS$^{\Delta}$PGSQFSK.W	**S284**	**4**	**0.99**	**30.66**	**6**	**0.99**	**57.5**	**-**
2: K.WPAS$^{\Delta}$PGSHSNDDFDNWSTFRPR.T	**S295**	**17**	**0.99**	**29.82**	**37**	**0.99**	**40.35**	**0.45**
3: R.TSSNASTISGRLS$^{\Delta}$PIMTEQDDLGDGDVHSLVYPPSAAK.M	**S326**	**33**	**0.90**	**30.65**	**20**	**0.60**	**24.89**	**1.65**
4: K.ELLTSDS$^{\Delta}$PPHNDIMSPVDPGVAQPNSR.V	**S467**	**5**	***0.34***	**16.22**	**13**	**0.59**	**12.09**	**0.38**
5: K.ELLTSDSPPHNDIMS$^{\Delta}$PVDPGVAQPNSR.V	**S475**	**5**	***0.34***	**32.44**	**10**	**0.72**	**44.72**	**0.5**
6: R.SCT$^{\Delta}$WPLPR.P	**T24**	**0**	**0**	**0**	**1**	**0.80**	**42.68**	**-**
7: K.SSWWMLNPEGGKSGKS$^{\Delta}$PR.R	**S246**	**2**	**0.99**	**16.23**	**5**	**0.99**	***10.49***	**-**
8: R.AAS$^{\Delta}$MDNNSKFAKSR.G	**S253**	**3**	**0.99**	**45.45**	**1**	**0.99**	**31.85**	**-**
9: C.YSFAPPNTSLNS$^{\Delta}$PSPNYSK.Y	**S413**	**0**	**0**	**0**	**1**	**0.31**	**14.42**	**-**
10: C.YSFAPPNTSLNSPS$^{\Delta}$PNYSK.Y	**S415**	**0**	**0**	**0**	**1**	**0.92**	***11.56***	**-**
11: R.TLPHVVNTMPHTSAMNRLT$^{\Delta}$PVK.T	**T553**	**2**	**0.99**	**37.41**	**1**	***0.36***	**12.03**	**-**

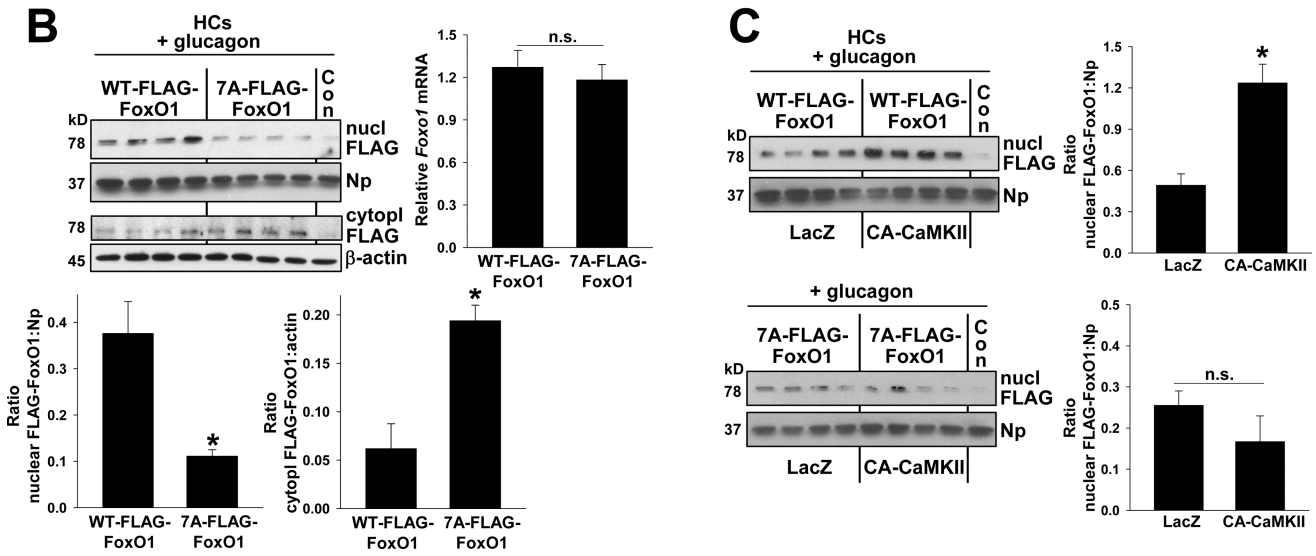

Figure 6. The role of non-AKT-phospho-sites of FoxO1 in CaMKII-mediated FoxO1 nuclear localization

(**A**) HCs from WT and *Camk2g*$^{-/-}$ mice were transduced with adeno-FLAG-FoxO1 at an MOI of 2. Cells were serum-depleted overnight and then incubated for 5 h in serumfree media. FoxO1 was immunopurified using anti-FLAG, followed by reduction, alkylation, and proteolytic digestion. Phosphorylated peptides were enriched by TiO_2 chromatography and then analyzed by LC-MS/MS as described in Experimental Procedures. The table shows spectral count number, Debunker score, and Ascore of phosphorylated peptides in KO and WT samples; Δ in the peptide sequence indicates the phosphorylation site. The cut-off values for spectral count #, Debunker score, and Ascore are set at 5, 0.5 and 12 respectively. The spectra of peptides with scores that are below these values (italics) were checked manually to eliminate uncertain phosphorylation sites (Figures S4A–B for WT peptides 4 and 5; and http://fields.scripps.edu/published/foxo1_Tabas_2012/ for KO peptides 7, 10, and 11). The KO/WT ratio of spectral counts was calculated only for peptides with a combined spectral count in KO and WT > 10. (**B**) HCs from L-FoxO1 mice were transfected with expression plasmids encoding murine Flag-FoxO1 or Flag-7A-FoxO1 mutant. After 48 h, the cells were serum-depleted overnight and then incubated with glucagon (100 nm) for 4 h in serum-free media. Nuclear extracts were assayed by immunoblot for Flag and nucleophosmin (nuclear loading control), and RNA from a parallel set of cells was probed for Foxo1 mRNA by RT-qPCR. Densitometric quantification of the mRNA and immunoblot data is shown in the graph (*P < 0.005; mean ± S.E.M.) (**C**) Similar to (B), except the HCs

were transduced with adeno-LacZ or CA-CaMKII one day after the transfection with the WT or mutant FoxO1 plasmids (*P = 0.003; mean ± S.E.M.).

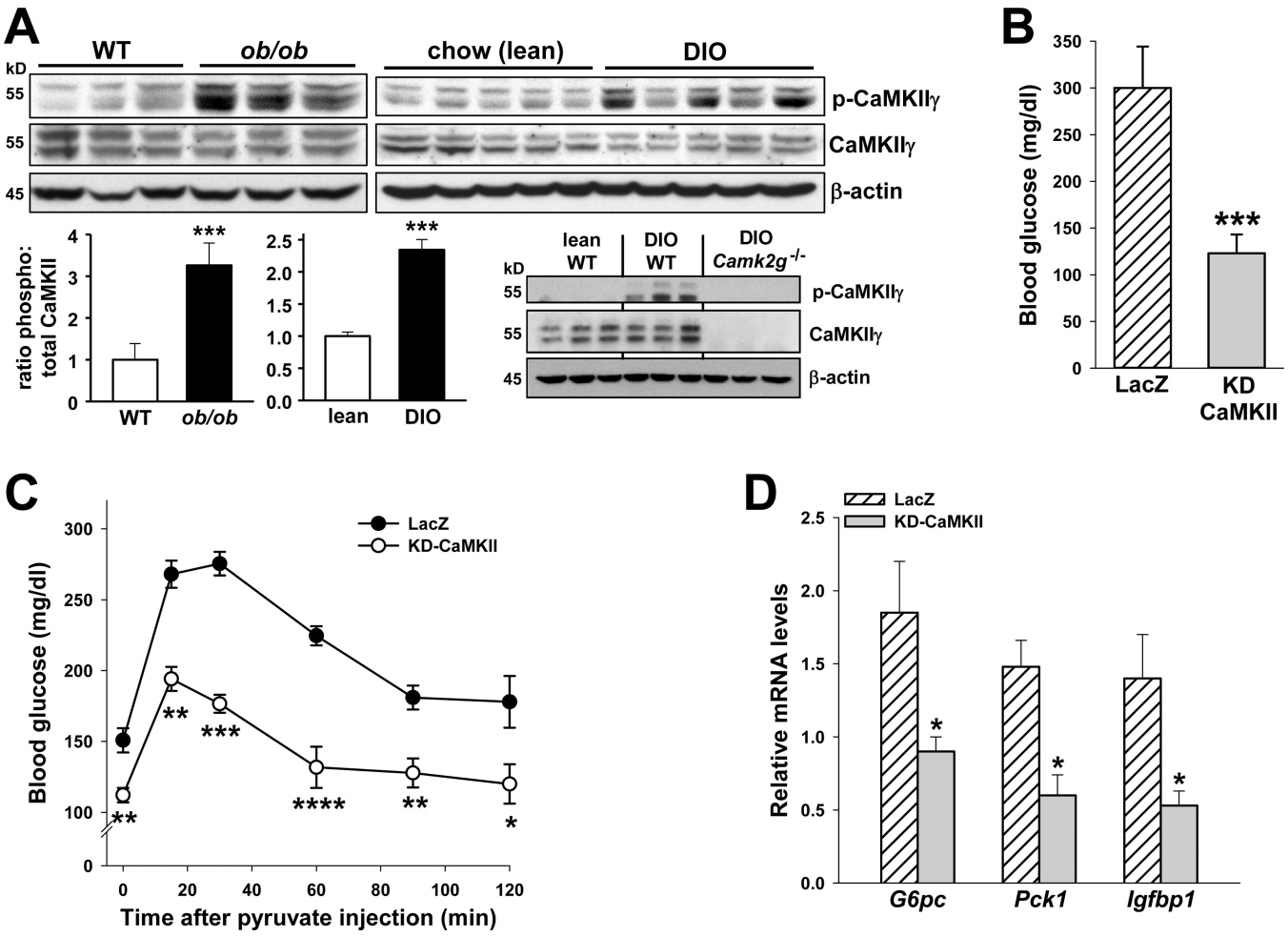

Figure 7. The role of CaMKII in hepatic glucose metabolism in obesity

(**A**) Liver extracts from 10-wk/o WT or *ob/ob* mice, or WT mice fed a chow or high-calorie diet for 20 wks (diet-induced obesity; DIO), were probed for p- and total CaMKIIγ and β-actin by immunoblot. Densitometric quantification is shown in the bar graph (***P < 0.001; mean ± S.E.M.). Antibody specificity is shown by the absence of p- and total CaMKIIγ bands in liver extracts from DIO *Camk2g*$^{-/-}$ mice. (**B–D)** Fasting blood glucose, blood glucose after pyruvate challenge, and liver *G6pc*, *Pck1* and *Igfbp1* mRNA in *ob/ob* mice before or after treatment with adeno-LacZ or KD-CaMKII (n = 5/group; *P < 0.05, **P < 0.01, ***P < 0.005, and ****P < 0.001 vs. LacZ; mean ± S.E.M.).